

The origin and history of ordinary chondrites: A study by iron isotope measurements of metal grains from ordinary chondrites

K.J. Theis^{a,*}, R. Burgess^a, I.C. Lyon^a, D.W. Sears^b

^a School of Earth, Atmospheric and Environmental Sciences, The University of Manchester, Manchester M13 9PL, UK

^b Arkansas Center for Space and Planetary Science and Department of Chemistry and Biochemistry, University of Arkansas, Fayetteville, AR 72701, USA

Received 15 August 2007; accepted in revised form 30 May 2008; available online 14 June 2008

Abstract

Chondrules and chondrites provide unique insights into early solar system origin and history, and iron plays a critical role in defining the properties of these objects. In order to understand the processes that formed chondrules and chondrites, and introduced isotopic fractionation of iron isotopes, we measured stable iron isotope ratios $^{56}\text{Fe}/^{54}\text{Fe}$ and $^{57}\text{Fe}/^{54}\text{Fe}$ in metal grains separated from 18 ordinary chondrites, of classes H, L and LL, ranging from petrographic types 3–6 using multi-collector inductively coupled plasma mass spectrometry. The $\delta^{56}\text{Fe}$ values range from -0.06 ± 0.01 to $+0.30 \pm 0.04\%$ and $\delta^{57}\text{Fe}$ values are -0.09 ± 0.02 to $+0.55 \pm 0.05\%$ (relative to IRMM-014 iron isotope standard). Where comparisons are possible, these data are in good agreement with published data. We found no systematic difference between falls and finds, suggesting that terrestrial weathering effects are not important in controlling the isotopic fractionations in our samples. We did find a trend in the $^{56}\text{Fe}/^{54}\text{Fe}$ and $^{57}\text{Fe}/^{54}\text{Fe}$ isotopic ratios along the series H, L and LL, with LL being isotopically heavier than H chondrites by $\sim 0.3\%$ suggesting that redox processes are fractionating the isotopes. The $^{56}\text{Fe}/^{54}\text{Fe}$ and $^{57}\text{Fe}/^{54}\text{Fe}$ ratios also increase with increasing petrologic type, which again could reflect redox changes during metamorphism and also a temperature dependant fractionation as meteorites cooled. Metal separated from chondrites is isotopically heavier by $\sim 0.31\%$ in $\delta^{56}\text{Fe}$ than chondrules from the same class, while bulk and matrix samples plot between chondrules and metal. Thus, as with so many chondrite properties, the bulk values appear to reflect the proportion of chondrules (more precisely the proportion of certain types of chondrule) to metal, whereas chondrule properties are largely determined by the redox conditions during chondrule formation. The chondrite assemblages we now observe were, therefore, formed as a closed system.

© 2008 Published by Elsevier Ltd.

1. INTRODUCTION

Iron, the ninth most abundant element in the universe, is found in chondritic meteorites in a variety of phases and redox states, making it a particularly important element in attempting to deduce chondrite origins, history and taxonomy.

The observation that iron occurs in three phases in chondritic meteorites (sulfide, metal and silicates) dates

to the very origins of modern meteorite research (Howard, 1802), but it was Prior (1916) who first described the oxidation-reduction trends in chondrites and pointed out their potential genetic significance. “Prior’s Laws” (the greater the FeO in the silicates the less the amount of metal and the higher that metal was in Ni) stood for almost 40 years, until Urey and Craig (1953) discovered that accompanying these oxidation or reduction trends, were changes in the total amount of Fe, the responsible process frequently being called the “metal-silicate fractionation”. This gave rise to the familiar major chondrite classes, such as H, L, LL.

To a large extent, understanding the origin and history of chondrites amounts to understanding their redox trends and metal-silicate fractionation (Sears, 2004). The redox

* Corresponding author.

E-mail address: karen.j.theis@postgrad.manchester.ac.uk (K.J. Theis).

trends are frequently assumed to be associated with chondrules—sub-millimetre spherules—some of which are refractory and highly reduced. The formation of large and abundant metal grains was probably also associated with chondrule formation (Larimer and Anders, 1967). Metal-silicate fractionation is frequently assumed to reflect the physical separation of metal and silicates. There are a wide variety of proposed mechanisms for both chondrule formation and metal-silicate fractionation, with very little consensus of opinion, but they can be broadly separated into those occurring in the nebula prior to agglomeration of the present rocks e.g., Wood (1963), Whipple (1966), Blander and Katz (1967), and Wasson (1972) and those that occur on the parent body e.g., Fredriksson (1963), Dodd (1971), Dodd (1981), Hutchison (2006) and Sears (2004). Nevertheless, chondrites are widely understood to be “cosmic sediments”, collections of diverse components that seem to owe their origins to a wide variety of processes in the early solar system.

Overlaid on the mineralogical and composition trends are meteorite-wide changes caused by processes such as aqueous alteration, thermal metamorphism and shock metamorphism. The most pervasive for the ordinary (H, L and LL) chondrites is thermal metamorphism, which is described in terms of petrographic types 3.0–3.9, 4, 5 and 6 (Van Schmus and Wood, 1967; Sears et al., 1980).

With the introduction of the high-resolution multi-collector inductively-coupled plasma mass spectrometer (MC-ICP-MS) it has become possible to measure the small natural variations in the iron isotope ratios of chondrites (e.g., Zhu et al., 2001). These isotopic properties hold the potential to shed new insights into the origin and history of these meteorites, and thus early solar system materials in general.

Critical to understanding the iron isotope fractionations in chondrites are laboratory data. Polyakov and Mineev (2000) used the second order Doppler (SOD) shift in the Mössbauer spectra from various iron minerals to determine the isotopic reduced partition function ratio as a function of temperature over the range of 0–1000 °C. Changes in $^{57}\text{Fe}/^{54}\text{Fe}$ by as much as 10‰ at 0 °C are predicted in some cases. Laboratory measurements of redox-related iron isotope fractionations have recently also been described (Anbar et al., 2000; Johnson et al., 2002; Welch et al., 2003), where $^{56}\text{Fe}/^{54}\text{Fe}$ fractionations of up to ~7‰ were observed.

Several authors have determined iron isotope ratios in meteorites in order to establish their initial solar nebula abundance, degree of homogeneity and to explore nebular processes (Zhu et al., 2000a; Alexander and Wang, 2001; Kehm et al., 2003; Mullane et al., 2005; Poitrasson et al., 2005; Poitrasson et al., 2006). Zhu et al. (2001), Kehm et al. (2003) and Mullane et al. (2005) reported Fe isotope fractionation in silicate phases of ordinary chondrites and found them to be enriched in the lighter isotopes compared with bulk fractions of the host meteorites and CI chondrite values. Alexander and Wang (2001) reported the iron isotope composition of olivines from individual chondrules and suggested that their wide range in forsterite content was not due to evaporation under Rayleigh conditions.

This would indicate an initial homogeneous iron reservoir with mass fractionation occurring during chondrule and parent body formation.

The present paper reports the first detailed measurements of the Fe isotope composition of metal grains separated from the major classes and petrographic types of ordinary chondrite meteorites. Preliminary reports of our work have been published as abstracts (Gildea et al., 2005, 2006, 2007). We investigate how Fe isotope composition of the metal grains relates to class and petrographic type, and assess whether terrestrial weathering has affected the primary Fe isotope ratios.

2. SAMPLES AND METHODS

2.1. Samples

Our samples were metal grains extracted from 18 chondritic meteorites: eleven H chondrites, six L chondrites and one LL chondrite. The samples range in petrographic types 3–6 and include falls and finds. The list of samples, their sources, catalogue numbers and other information is given in Table 1. Except for Barwell, the metal grains were obtained as magnetic separates that were originally prepared for thermoluminescence studies (Sears and Mills, 1974; Sears and Durrani, 1980) and metallographic studies (Sears and Axon, 1975; Sears and Axon, 1976). The original samples were from the interior portions of the meteorites in order to avoid any obvious terrestrially contaminated and weathered material, or material altered by atmospheric passage. The Barwell sample consisted of chips that were then crushed and the metal removed for this study. The hand-picked metal grains were examined under a microscope and appeared to be free of signs of oxidation.

2.2. Sample preparation and dissolution

The metal grains were further purified by crushing under acetone with an agate mortar and pestle, and then hand-picked with the aid of a binocular microscope to be visibly free of any adhering silicate material. The metal grains were then dissolved in 10% nitric acid solution on a hot plate (at ~50 °C). Once the solutions had cooled they were then diluted with 18.2 MΩ water to reduce the nitric acid concentration to 2%.

Previous analyses of Fe isotope ratios in meteorite samples have used chromatography to separate iron from other elements that were also present in the solutions. Elements that may cause analytical difficulties for the precise determination of Fe isotope ratios are those that cause mass interferences such as ^{54}Cr which is isobaric with ^{54}Fe or elements such as Mg and Ca which in solution can change plasma conditions in the MC-ICP-MS instrument causing variable instrumental fractionation (i.e. matrix effects, Kehm et al., 2003).

However, chromatographic separation of iron can induce fractionation of Fe isotopes which could mask any Fe isotope fractionation inherent in the samples (Anbar et al., 2000). We therefore wished to avoid chromatographic techniques and used a method which dissolved the iron grains

Table 1
Samples analysed in this study

Samples	Source and Catalogue no. (where known)	Class	Fe/Si (m) (a/a)	Fe/Si (sil + sul) (a/a)	References	Sample size μg
Bremervörde	BM33910	H3	0.35	0.44	[4]	32
Clovis (No. 1)	USNM 2170	H3	0.41	0.38	[3], [6]	57
Beaver Creek	BM73646	H4	0.54	0.35	[2], [6], [7]	27
Elm Creek	S and H	H4	0	0.66	[6]	75
Faucett	S and H	H4	0.44	0.44	[6], [11]	159
Acme		H5	No data	No data		7
Gilgoin	S and H	H5	No data	No data	[6]	759
Jilin	CAS	H5	0.73	0.39	[12]	126
Plainview (1917)	BM1959,805	H5	0.43	0.46	[6], [14]	130
Estacado	S and H	H6	0.49	0.40	[6], [7]	254
Kernouve	BM43400	H6	0.64	0.31	[6], [7], [13]	60
Bluff (a)		L5	0.19	0.44	[8]	29
Crumlin	BM86115	L5	0.22	0.42	[1], [6], [9]	92
Etter	AML	L5	0.12	0.50	[6], [10]	6
Barwell	BM1965,57	L6	0.16	0.43	[5], [6]	456
Calliham	AML	L6	No data	No data	[6]	2
De Nova	S and H	L6	No data	No data	[6]	169
Aldsworth	BM61308	LL5	0.01	0.52	[1]	3

BM, British Museum, Natural History; CAS, Chinese Academy of Sciences; Guiyang, China. USNM, National Museum of Natural History, Smithsonian Institution, Washington, D.C.; AML, Dr. G Huss, American Meteorite Lab. S and H, Prof H.E. Suess and Dr. M. Hendon. [1] (Sears and Mills, 1974) [2] (Sears et al., 1980) [3] (Jarosewich, 1966) [4] (Dodds et al., 1967) [5] (Jobbins et al., 1966) [6] (Sears and Durrani, 1980) [7] (Urey and Craig, 1953) [8] (Mason and Wiik, 1967) [9] (Jarosewich and Dodd, 1985) [10] (Rubin et al., 1983) [11] (King et al., 1977) [12] (Yanai et al., 1995) [13] (Hutchison et al., 1981) [14] (Fodor and Keil, 1976).

taking the minimum of other elements into solution. Matrix effects from elements other than iron in solution and their evaluation are described in the next section.

2.3. MC-ICP-MS analysis

$^{56}\text{Fe}/^{54}\text{Fe}$ and $^{57}\text{Fe}/^{54}\text{Fe}$ isotopic ratios were determined using a Nu Instruments high resolution (HR) double focusing multi-collector inductively-coupled plasma mass spectrometer (MC-ICP-MS). Sample solutions were introduced with a CETAC ASX-100 auto-sampler and Nu Instruments DSN-100 desolvating nebuliser to reduce isobaric interferences from ArN^+ (which interferes with ^{54}Fe), ArO^+ (^{56}Fe) and ArOH^+ (^{57}Fe) ions. These interferences were further reduced by operating the MC-ICP-MS in pseudo high resolution by decreasing the entrance slit to $\sim 30\mu\text{m}$. This is sufficient to ensure that the iron isotopes and the interfering isobaric interferences are resolved as flat topped peaks with iron ‘shoulders’ to the low mass side of the peak (Weyer and Schwieters, 2003). Elemental interferences, such as ^{54}Cr , were monitored and corrected for by monitoring ^{53}Cr and assuming a terrestrial ratio of $^{54}\text{Cr}/^{53}\text{Cr} = 0.2489$. Levels of chromium were monitored during Fe isotopic analysis and found to be negligible.

The Fe isotopic data are reported using the conventional delta notation, relative to the IRMM-014 iron isotope standard (Institute of Reference Materials JRC Reference Laboratory for Isotopic Measurements $^{56}\text{Fe}/^{54}\text{Fe} = 15.69786$, $^{57}\text{Fe}/^{54}\text{Fe} = 0.36257$):

$$\delta^{56}\text{Fe} = \left[\left(\frac{^{56}\text{Fe}/^{54}\text{Fe}_{\text{sample}}}{^{56}\text{Fe}/^{54}\text{Fe}_{\text{standard}}} \right) - 1 \right] \times 1000$$

and

$$\delta^{57}\text{Fe} = \left[\left(\frac{^{57}\text{Fe}/^{54}\text{Fe}_{\text{sample}}}{^{57}\text{Fe}/^{54}\text{Fe}_{\text{standard}}} \right) - 1 \right] \times 1000$$

where $^{x}\text{Fe}/^{54}\text{Fe}_{\text{sample}}$ and $^{x}\text{Fe}/^{54}\text{Fe}_{\text{standard}}$ refer to the isotopic ratios for sample and IRMM-014 standard, respectively.

2.4. Fe isotope measurements

The sample-standard bracketing method (Belshaw et al., 2000) was used to correct for possible instrumental fractionation with 5–6 sample-standard measurements made for each analysis.

Both standard and sample were signal strength matched to within 10% using 1 and 2 ppm solutions. Acid washes, used to prevent sample-standard crossover, were checked for iron content after analysis and found to contain less than 1 ppb. Prior to measurements, the analyte was allowed 110 s to equilibrate and stabilise before beginning data acquisition. Each analyte measurement began with mass scanning at m/z 54 to locate the low mass ^{54}Fe shoulder. Zero readings were measured while deflecting the ion beams away from the collector region by increasing the ESA voltage. Following this 50 readings were taken using 3 s integration times at m/z 53 (Cr), 54, 56 and 57 using Faraday detectors.

For each sample analysed, the mean isotopic ratios and standard errors were calculated from each set of 5–6 sample/standard measurements, and repeat analysis of some samples was carried out 2–3 times throughout the study period. All Fe isotope values are reported relative to the IRMM-014 iron isotope standard (which is -0.09 and -0.11‰ relative to bulk Earth for $\delta^{56}\text{Fe}$ and $\delta^{57}\text{Fe}$, respectively (Beard and Johnson, 2004a)). Errors reported in this work are 2σ standard errors of multiple measurements made on each sample of the difference between the sample and the standard. These were typically in the range 0.02 – 0.11‰ in $\delta^{56}\text{Fe}$.

Table 2

External reproducibility for Fe isotope analyses between the JM Fe standard and the IRMM014 Fe isotope standard for period 2005/2006

Method	$\delta^{56}\text{Fe}$ (‰)	SD (1 σ)	$\delta^{57}\text{Fe}$ (‰)	SD (1 σ)
Average 'dry' plasma at 1 ppm for 2005	0.35	0.07	0.52	0.17
Average 'wet' plasma at 5 ppm for 2005	0.35	0.05	0.50	0.08
Average 'dry' plasma at 1 ppm for 2006	0.34	0.06	0.52	0.06

'Dry' plasma refers to the analyte being introduced by desolvating nebuliser to reduce the carrier solution (2% HNO₃) and thereby moderate isobaric interferences. Wet plasma refers to the analyte being introduced straight into the spray chamber.

The long term reproducibility of the MC-ICP-MS has been monitored by analysing a Johnson–Matthey Plc (JM) Fe internal standard against the IRMM-014 Fe isotope standard and the results are summarised in Table 2. Results are shown for measurements using both a conventional spray chamber ('wet' plasma) and desolvating nebuliser ('dry' plasma) to compare plasma conditions, however all samples analysed in this study were obtained under dry plasma conditions. Over a two and half year period of continuous operation, these measurements give mean and standard errors (2 σ) of $\delta^{56}\text{Fe} = 0.35 \pm 0.02\%$ and $\delta^{57}\text{Fe} = 0.51 \pm 0.02\%$.

2.5. Sample purity and matrix corrections

2.5.1. Sulphides

Troilite (FeS) is a possible contaminant in the Fe grains and there is isotopic fractionation of iron in sulphides compared to metallic iron (Poitrasson et al., 2005; Weyer et al., 2005, 2007; Needham et al., 2006; Poitrasson, 2007). It was, therefore, important to determine whether there was a significant sulphide content in any of the metal grains. During the preparation phase any grains showing a yellow colouration were discarded and no sulphurous (e.g. H₂S, SO₂) odour was observed during dissolution, a very sensitive test. To more accurately assess whether sulphide was present, a fraction of the hand picked metal grains was separated for each class and petrographic type of meteorite and prepared for compositional analysis by scanning electron microscopy. The grains were mounted on glass slides using resin and their surfaces were polished to reveal fresh metal. The scanning electron microscope used for this analysis was the Philips XL30 Environmental Scanning Electron Microscope FEG at 20 kV. Metal grains from Bremervörde (H3), Faucett (H4), Gilgoin (H5), Estacado (H6), Crumlin (L5) and Barwell (L6) were analysed to determine whether any of the metal grains may have contained sulphides. Numerous spot analyses conducted on each grain revealed that the only metal phases present in all six meteorite samples were kamacite and taenite.

2.5.2. Matrix effects

It was not possible to obtain pure metal separates due to the fine-scale of silicate-metal intergrowth and we did not want to purify the samples by anion exchange chromatography due to isotopic fractionation that is possible in the column (Anbar et al., 2000). The presence of other cations influences Fe isotope fractionation in the MC-ICP-MS by matrix effects so it is important to quantify the level of this effect.

Fe isotope fractionation was measured in solutions of our internal Fe isotope standard (JM) mixed with Mg to give Mg/Fe v/v ratios of between 2 and 0.1. The results are displayed in Fig. 1a and b and show a linear decrease in $\delta^{56}\text{Fe}$ and $\delta^{57}\text{Fe}$ with Mg/Fe ratio. Thus, Fe isotope ratios from the meteorite samples can be corrected once the Mg concentration of the solution is known. For example correction of $\delta^{56}\text{Fe}$ is given by:

$$\delta^{56}\text{Fe} = \delta^{56}\text{Fe}_{\text{meas}} - (\delta^{56}\text{Fe}_{\text{meas}} + m^* \text{Mg}/\text{Fe}_{\text{meas}}) \quad (1)$$

Where $\delta^{56}\text{Fe}_{\text{meas}}$ and $\text{Mg}/\text{Fe}_{\text{meas}}$ are the measured $\delta^{56}\text{Fe}$ and Mg/Fe ratio of the sample and $m = 0.342$, the slope of the correlation in Fig. 1a. In fact, most sample Mg/Fe ratios were found to be low from 4×10^{-2} to 5×10^{-5} , requiring an insignificant correction ($<0.01\%$ $\delta^{56}\text{Fe}$). Two exceptions were Calliham and Etter both having Mg/Fe = 0.1 which required corrections to $\delta^{56}\text{Fe}$ and $\delta^{57}\text{Fe}$ of 0.06 and 0.1‰, respectively.

Similar matrix effects are also caused by the presence of Ni and Co within the sample solutions. In order to ascertain whether any corrections should also be applied based on the concentrations of Ni and Co present within the samples, similar experiments to those done with Mg were carried-out using a JM nickel standard and a JM cobalt standard.

The results showed that increasing the concentrations of Ni and Co reduces the Fe isotope ratio, so that the iron isotope compositions are apparently more enriched in the lighter isotopes. Fig. 1c and d show the negative correlation between (Co + Ni)/Fe ratio and iron isotope composition, however, the trend for $\delta^{56}\text{Fe}$ is much stronger than for $\delta^{57}\text{Fe}$. If this is a matrix effect and, therefore, mass dependant, $\delta^{57}\text{Fe}$ should be affected by $1.5 \times \delta^{56}\text{Fe}$. Although this does not appear to be the case for $\delta^{57}\text{Fe}$ we have assumed that the reason for this is due to the increase in error given that $\delta^{57}\text{Fe}$ is much less abundant and more prone to interference and noise. The correction to measured $\delta^{56}\text{Fe}$ for matrix effects from Co and Ni has been carried out using an average of the slope (m) of the correlation in Fig. 1c and the slope (m) in Fig. 1d (multiplied by 0.75 assuming mass dependant fractionation, as $\delta^{56}\text{Fe}$ shows a correlation but $\delta^{57}\text{Fe}$ does not) and the measured (Co+Ni)/Fe ratio of the sample using an analogous correction to Eq. (1). The same was done for $\delta^{57}\text{Fe}$ with the slope obtained for the (Co+Ni)/Fe vs $\delta^{56}\text{Fe}$ correlation being an average of both the $\delta^{57}\text{Fe}$ and $\delta^{56}\text{Fe}$ (multiplied by 1.5 assuming mass dependent fractionation).

Table 3 shows the concentrations of Mg, Co and Ni present in the meteorite samples and gives their ratio relative to Fe. However, only Calliham and Aldsworth contained significant Co and Ni contents with (Co+Ni)/Fe

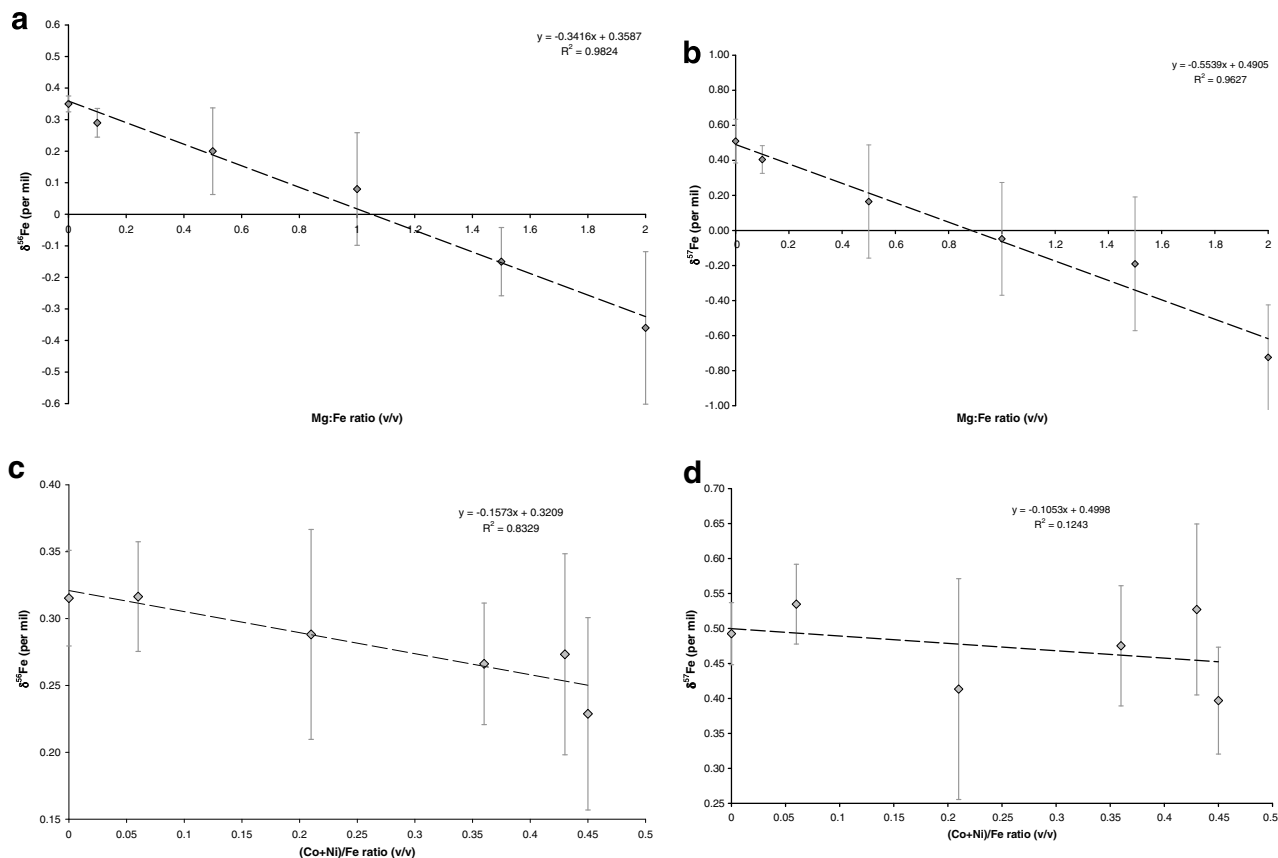


Fig. 1. The effect of varying the Mg/Fe and (Co+Ni)/Fe ratios in solution on the iron isotope ratios. The ratios were volumetrically determined using mixtures of Johnson–Matthey Mg, Ni, Co and Fe standards relative to the IRMM014 iron isotope standard. The influence of the Mg causes a negative linear correlation between (a) the $\delta^{56}\text{Fe}$ values and (b) $\delta^{57}\text{Fe}$ values, with increasing Mg/Fe value. Error bars are to 2σ . The influence of Co and Ni also causes a negative linear correlation between (c) $\delta^{56}\text{Fe}$ values and (d) $\delta^{57}\text{Fe}$ values. This implies that for samples with a Mg/Fe ratio ≤ 0.1 and (Co+Ni)/Fe ratio < 0.32 the iron isotope composition does not need to be corrected for but anything over these ratios the isotope ratio can be re-calculated accordingly.

ratios of >0.358 , thus requiring a correction of $+0.04\text{‰}$ and $+0.05\text{‰}$, respectively, for $\delta^{56}\text{Fe}$ and $+0.07\text{‰}$ for both samples for $\delta^{57}\text{Fe}$.

3. RESULTS

The results are listed in Table 4 and plotted as a three-isotope diagram in Fig. 2. Some meteorites were analysed 2–3 times over the course of the analytical period. For these samples the error weighted mean isotopic values have been calculated and are considered the most representative value. Results shown in Table 4 include data for individual runs as well as average values. Out of the eleven samples that were repeated, four show reproducibilities in $\delta^{56}\text{Fe}$ of 0.08–0.17‰, one shows a difference of 0.05‰, and six vary by only 0.02‰ or less (Table 4).

With the exception of Bluff (a), the $\delta^{56}\text{Fe}$ values range from $-0.02 \pm 0.01\text{‰}$ to $+0.30 \pm 0.04\text{‰}$ and our $\delta^{57}\text{Fe}$ values range from $-0.03 \pm 0.06\text{‰}$ to $+0.55 \pm 0.05\text{‰}$. Bluff (a) is an L5 and has the lowest iron isotope values measured of the entire sample set, with a $\delta^{56}\text{Fe}$ of $-0.06 \pm 0.01\text{‰}$, and a $\delta^{57}\text{Fe}$ of $-0.09 \pm 0.02\text{‰}$. The results from this sample are discussed separately below.

Fig. 2 shows a plot of $\delta^{56}\text{Fe}$ vs. $\delta^{57}\text{Fe}$ for iron grains from all meteorites. The data define a linear correlation with slope 1.50 ± 0.24 , within error of the expected slope of 1.48 for the mass fractionation line for this system. There is no evidence for the presence of radiogenic or nucleosynthetic components in this stable isotope system.

$\delta^{56}\text{Fe}$ values of meteorite falls of $-0.02 \pm 0.01\text{‰}$ to $+0.30 \pm 0.02\text{‰}$, and $\delta^{57}\text{Fe}$ values of $-0.03 \pm 0.06\text{‰}$ to $+0.49 \pm 0.09\text{‰}$ are similar to the ranges for finds of $\delta^{56}\text{Fe}$ from $+0.01 \pm 0.01\text{‰}$ to $+0.30 \pm 0.04\text{‰}$ and $\delta^{57}\text{Fe}$ from $-0.01 \pm 0.05\text{‰}$ to $+0.55 \pm 0.05\text{‰}$. The lack of any isotopic difference between falls and finds indicates that weathering is not affecting iron isotopic composition of the metal phase.

There does, however, appear to be a relationship between chemical class and iron isotope composition with increasing $\delta^{56}\text{Fe}$ and $\delta^{57}\text{Fe}$ in order of $\text{H} < \text{L} < \text{LL}$ (Fig. 3). There is also a relationship between petrographic type and iron isotope composition with $\delta^{56}\text{Fe}$ and $\delta^{57}\text{Fe}$ values increasing in order of $3 < 4 < 5 < 6$ (Fig. 4). However, metal from type 6 chondrites shows the widest range of Fe isotope values with $\delta^{56}\text{Fe}$ between $-0.02 \pm 0.01\text{‰}$ and $+0.30 \pm 0.04\text{‰}$ and $\delta^{57}\text{Fe}$ between $-0.03 \pm 0.06\text{‰}$ and $+0.55 \pm 0.05\text{‰}$.

Table 3
Concentrations of matrix elements (Mg, Co and Ni) present in sample solutions and their ratio relative to Fe

Meteorite	Fe (ppm)	Mg (ppb)	Mg/Fe ratio	Co (ppb)	Ni (ppb)	(Co + Ni)/Fe
Bremervörde H3	1.4	27.10	0.019	7.81	183.16	0.14
Clovis (No. 1) H3	2.6	33.48	0.013	14.82	277.92	0.11
Beaver Creek H4	1.3	24.82	0.019	6.68	198.15	0.16
Elm Creek H4	4.0	61.90	0.015	23.90	387.91	0.10
Faucett H4	2.1	41.27	0.020	11.94	235.41	0.12
Acme H5	1.1	27.10	0.025	12.72	248.75	0.24
Gilgoi H5	2.3	63.26	0.028	12.55	232.18	0.11
Jilin H5	2.3	63.64	0.028	12.05	220.25	0.10
Plainview (1917) H5	2.2	41.73	0.019	13.06	247.87	0.12
Estacado H6	2.4	27.88	0.012	13.31	247.15	0.11
Kernouve H6	2.7	25.62	0.009	14.58	303.65	0.12
Bluff (a) L5	2.5	36.21	0.014	15.62	568.21	0.23
Crumlin L5	2.4	45.00	0.019	18.35	511.93	0.22
Etter L5 ^a	1.2	72.29	0.060	10.20	230.15	0.20
Barwell L6	2.1	42.33	0.020	19.96	241.96	0.12
Calliham L6 ^a	1.1	69.86	0.064	85.58	350.91	0.40
De Nova L6	2.5	32.69	0.013	21.25	292.85	0.13
Aldsworth LL5 ^a	1.3	27.99	0.022	23.65	453.81	0.37

^a Samples, where a correction to $\delta^{56}\text{Fe}$ and $\delta^{57}\text{Fe}$ was applied for effects of matrix elements on iron isotope composition.

4. DISCUSSION

Fig. 5 is a diagrammatic representation of our data sorted by meteorite class and petrographic type. Trends are evident as the meteorite isotopic compositions increase from H through L to LL and also from petrographic type 3–6. There are a number of processes that may explain these trends and we will discuss them in terms of the effects of weathering, chemical class and petrographic type.

Following Van Schmus and Wood (1967), chondritic meteorites are considered to be uniquely described by a combination of chemical class and petrographic type, although other parameters (such as shock stage) are occasionally included. This classification, although purely descriptive, is widely thought to capture the critical elements of chondrite formation and history. All data discussed from this point will refer only to the $\delta^{56}\text{Fe}$ values as these are most commonly reported in previous studies of iron isotopes in meteorites. In any event, $\delta^{57}\text{Fe}$ and $\delta^{56}\text{Fe}$ are linearly related (Fig. 2), so $\delta^{57}\text{Fe}$ may be readily inferred from the $\delta^{56}\text{Fe}$ value.

4.1. Weathering

Weathering is a perpetual problem in studies of all finds and some falls and is a particular challenge with respect to the large numbers of meteorites being found in the hot and cold deserts (Bland, 2006). While there do not appear to be systematic effects in $\delta^{56}\text{Fe}$ composition between falls and finds analysed here, it is instructive to consider the magnitude of the isotope effects associated with terrestrial weathering and their possible influence on the primary composition of the metal grains in chondrites.

Weathering causes the oxidation and hydrolysis of metal and sulphide, and it leaches certain elements from the whole rock. The analysis of Mössbauer data for iron minerals by Polyakov and Mineev (2000) predicts that isotopic fraction-

ation between ferric and ferrous Fe-bearing species at low temperatures could be as much as $\sim 10\%$. Fig. 6a shows the inter-mineral fractionation between iron and goethite and also olivine and goethite at $\sim 25^\circ\text{C}$. The plot indicates that an expected equilibrium fractionation of at least $+0.58\%$ in the case of iron to goethite and $+1.51\%$ between olivine and goethite should be present if terrestrial weathering had caused any fractionation of the iron isotopes. Fig. 6b shows the temperature dependence of the fractionation partition coefficients for a number of different minerals commonly found in meteorites. Both plots are based on data in Polyakov and Mineev (2000).

Laboratory experiments by Johnson et al. (2002) and Welch et al. (2003), showed differences of $\sim 3.0\%$ during equilibrium fractionation between aqueous Fe(II) and Fe(III). Anbar et al. (2000) showed that incomplete extraction of iron during ion-exchange chromatography of FeCl complexes could also fractionate the iron isotopes by a few per mil. Early fractions were enriched in the heavier isotope ($\delta^{56}\text{Fe} > 0$) while later fractions were depleted ($\delta^{56}\text{Fe} < 0$). Overall differences of 3.6 to -3.4% were observed. However, fractionation obtained from experimental data appear to be much smaller than those calculated by Polyakov and Mineev (2000), with the amount of fractionation dependant on the partitioning process, rate, pH and temperature. Measured effects are on the order of $\delta^{56}\text{Fe} \sim 4\%$ for natural systems (Zhu et al., 2000b; Beard et al., 2003; Johnson et al., 2003; Anbar, 2004; Beard and Johnson, 2004b). We are unaware of any iron isotope studies of chondrite weathering, but in terrestrial systems, in the absence of metal, weathering does appear to result in small fractionations in $\delta^{56}\text{Fe}$ (Fantle and DePaolo, 2004; Bergquist and Boyle, 2006).

Neglecting leaching, we can consider weathering to be described as

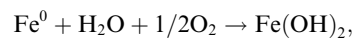
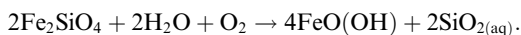


Table 4
Fe isotope data with 2σ uncertainties

Meteorite sample	Class/Pet-Type/Fall or Find	$\delta^{56}\text{Fe}$	2σ	$\delta^{57}\text{Fe}$	2σ
Bremervorde	H3 Fall	−0.01	0.07	−0.02	0.11
Clovis (No. 1)	H3 Find	0.01	0.02	−0.09	0.12
Clovis (No. 1) (d)	H3 Find	0.03	0.05	0.04	0.08
Clovis (No. 1) ave	H3 Find	0.01	0.01	−0.01	0.05
Beaver Creek	H4 Fall	0.08	0.07	0.12	0.16
Beaver Creek (d)	H4 Fall	0.07	0.07	0.17	0.13
Beaver Creek ave	H4 Fall	0.08	0.03	0.15	0.07
Elm Creek	H4 Find	0.12	0.04	0.21	0.10
Elm Creek (d)	H4 Find	0.12	0.05	0.22	0.09
Elm Creek ave	H4 Find	0.12	0.02	0.21	0.04
Faucett	H4 Find	0.08	0.04	0.04	0.15
Faucett (d)	H4 Find	0.06	0.11	0.15	0.04
Faucett ave	H4 Find	0.08	0.03	0.14	0.03
Acme	H5 Find	0.19	0.09	0.27	0.11
Acme (d)	H5 Find	0.08	0.03	0.10	0.04
Acme ave	H5 Find	0.10	0.02	0.12	0.03
Gilgoin	H5 Find	0.12	0.03	0.15	0.03
Jilin	H5 Fall	0.06	0.02	0.19	0.09
Jilin (d)	H5 Fall	0.11	0.04	0.23	0.08
Jilin ave	H5 Fall	0.07	0.02	0.21	0.04
Plainview (1917)	H5 Find	0.10	0.11	0.20	0.31
Plainview (1917) (d)	H5 Find	0.09	0.02	0.17	0.07
Plainview (1917) ave	H5 Find	0.09	0.02	0.17	0.06
Estacado	H6 Find	0.13	0.07	0.21	0.11
Kernouve	H6 Fall	−0.01	0.03	0.02	0.18
Kernouve (d)	H6 Fall	−0.03	0.02	−0.04	0.09
Kernouve ave	H6 Fall	−0.02	0.01	−0.03	0.06
Bluff (a)	L5 Find	−0.09	0.05	−0.04	0.18
Bluff (a) (d)	L5 Find	−0.01	0.06	−0.01	0.11
Bluff (a) (d)	L5 Find	−0.07	0.02	−0.11	0.04
Bluff (a) ave	L5 Find	−0.06	0.01	−0.09	0.02
Crumlin	L5 Fall	0.19	0.05	0.36	0.11
Crumlin (d)	L5 Fall	0.06	0.06	0.13	0.09
Crumlin ave	L5 Fall	0.14	0.03	0.23	0.05
Etter*	L5 Find	0.25	0.05	0.46	0.04
Barwell	L6 Fall	0.33	0.04	0.55	0.16
Barwell (d)	L6 Fall	0.16	0.08	0.22	0.12
Barwell ave	L6 Fall	0.30	0.02	0.34	0.10
Calliham*	L6 Find	0.30	0.04	0.55	0.05
De Nova	L6 Find	0.21	0.02	0.32	0.09
Aldsworth*	LL5 Fall	0.28	0.07	0.49	0.09

The bold entries reflect the calculated error weighted mean for meteorites which have more than one individual set of measurements and they are also the data that have been plotted in Fig. 2. (d, duplicate of sample re-analysed at different time; ave, average result error weight corrected; * isotopic ratio correction applied for matrix effects).

and Fe silicate oxidation:



Fractionation of iron isotopes caused by weathering should therefore be readily detectable within experimental uncertainties. Yet we see little or no evidence for this in that falls and finds do not show consistent differences in Fe isotope composition. We presume this is because either the iron grains were unweathered, having been selected from interior portions of the meteorites, or that the iron isotope system was effectively closed during weathering and sample preparation, with any weathering products being fully sampled during acid dissolution. The lack of any significant difference in Fe isotope ratios between falls and finds suggests that weathering has not had a major influence on the data.

4.2. Chemical classes

As discussed above, Prior (1916) and Urey and Craig (1953) have given us the modern chondrite classification scheme which embraces the dual effects of decreasing metal and increasing oxidation along the series H → L → LL. This is shown in Fig. 7, with the present samples—where data are available—also plotted.

We observe an increase in $\delta^{56}\text{Fe}$ and $\delta^{57}\text{Fe}$ values along the series H → L ≈ LL suggesting that iron isotopes were fractionated during metal silicate fractionation, or by increasing oxidation/reduction of iron (Fig. 3). We will first discuss the metal-silicate fractionation and then the oxidation process as possible causes of iron isotope fractionation.

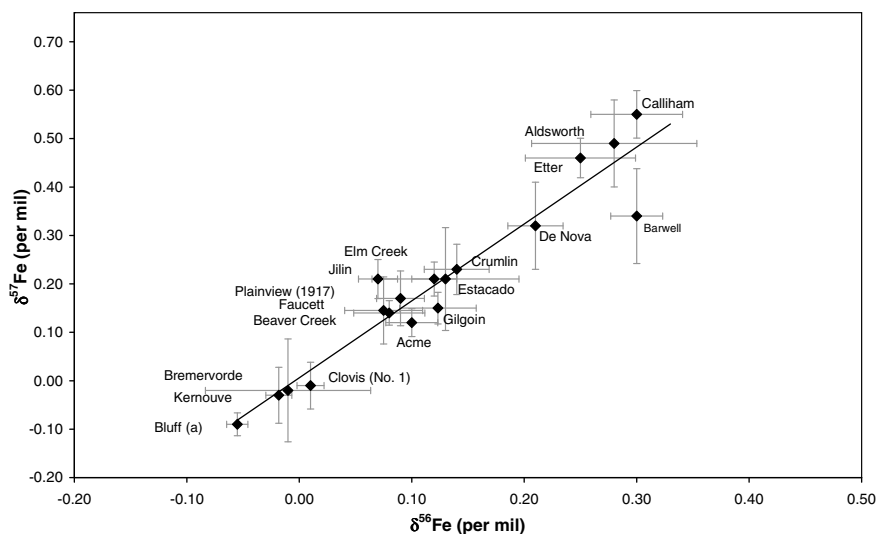
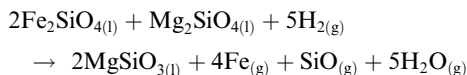


Fig. 2. $\delta^{57}\text{Fe}$ – $\delta^{56}\text{Fe}$ three isotope plot for metal grains in ordinary chondrites. Error bars shown at 2σ uncertainty. The mass fractionation line shown has a slope of 1.50 ± 0.24 indicating no evidence for the presence of radiogenic or nucleosynthetic components. See text for discussion.

Urey and Craig (1953) originally suggested that metal-silicate fractionation was the igneous process of differentiation. Subsequent workers have recognized that chondrites are not igneous products but sediments of highly diverse primary components. Thus, a number of mechanisms for separating metal and silicate without melting have been proposed. All rely on the physical properties of metal and silicates, such as magnetism, ductility, grain size, and density (Donn and Sears, 1963; Whipple, 1966; Harris and Tozer, 1967; Orowan, 1969; Larimer and Anders, 1970; Rowe et al., 1972; Dodd, 1976a; Dodd, 1976b; Weidenschilling, 1977). More recently, Huang et al. (1996) and Akridge and Sears (1999) suggested that gravity and density sorting in a thick regolith of a small asteroid would produce metal-silicate separations of the sort observed in the ordinary chondrites. These physical processes would separate the iron from the silicates without undergoing chemical changes and would not result in the isotopic fractionations observed in Fig. 3.

The oxidation state differences between the classes are thought to reflect the reduction of Fe-rich silicates to metallic iron, most probably associated with the formation of chondrules. Such reactions as:



are thought to take place during chondrule formation and result in the formation of metallic iron, as fine dusty grains that coagulate into larger particles during secondary events.

The fractionation of iron isotopes during this process is not well-known, but the data from Polyakov and Mineev (2000), (Fig. 6b), can be used to estimate the expected isotopic variation (depending on temperature) for Fe^{2+} silicates relative to metallic iron. At low temperatures ($\sim 15^\circ\text{C}$), the isotopic difference $\Delta^{56}\text{Fe}$ between enstatite and metal iron is predicted to be as much as $+2\text{‰}$. At higher temperatures of $1500^\circ\text{C}+$ (shown in Fig. 8), the isotopic

partition function is approaching equilibrium and $\Delta^{56}\text{Fe}$ is, therefore, much smaller—only 0.02‰ for enstatite-metal iron fractionation and 0.0‰ for diopside—metal iron, the former being just resolvable within the precision of the Fe isotope measurements.

Fig. 5 shows how the isotopic compositions of the meteorites increase through each of the three groups. The data set which shows this most clearly is from type 5 meteorites since it is the most complete. Meteorite class H has an average $\delta^{56}\text{Fe}$ of 0.09‰ , L (excluding Bluff (a)) has an average $\delta^{56}\text{Fe}$ of 0.2‰ and the only LL sample has a $\delta^{56}\text{Fe}$ of 0.28‰ . The overall variation is 0.18‰ which would seem consistent with the formation of metal by the reduction of silicates and not simply temperature dependant fractionation. There is also some experimental data on this topic, Roskosz et al. (2006) produced metallic iron by the reduction of a silicate melt and found that at sub-liquidus temperatures the metal iron is initially enriched in the lighter iron isotope as kinetics govern the fractionation before the system finally reaches a state of equilibrium in which the metal iron is isotopically heavier than the remaining silicate melt by $+0.2 \pm 0.15\text{‰/amu}$. Thus both the Mössbauer data and the Roskosz et al. (2006) experimental data are consistent with reduction during chondrule formation being the cause of the isotopic fractionation as observed between Fe in metal and chondrules.

4.3. Petrographic type

Chondrites respond to metamorphism in many ways. Heterogeneous minerals become homogeneous, fine grains of dusty metal and sulphide coarsen to become large intergrown grains, glass can crystallize to produce feldspar and mafic minerals and water and inert gases can be lost. These qualitative changes are recognized in the petrographic types 3–6, for which various geothermometers suggest the following closure temperatures: type 3, $<600^\circ\text{C}$; type 4, $600\text{--}700^\circ\text{C}$; type 5, $700\text{--}750^\circ\text{C}$; type 6, $750\text{--}950^\circ\text{C}$ (McSween

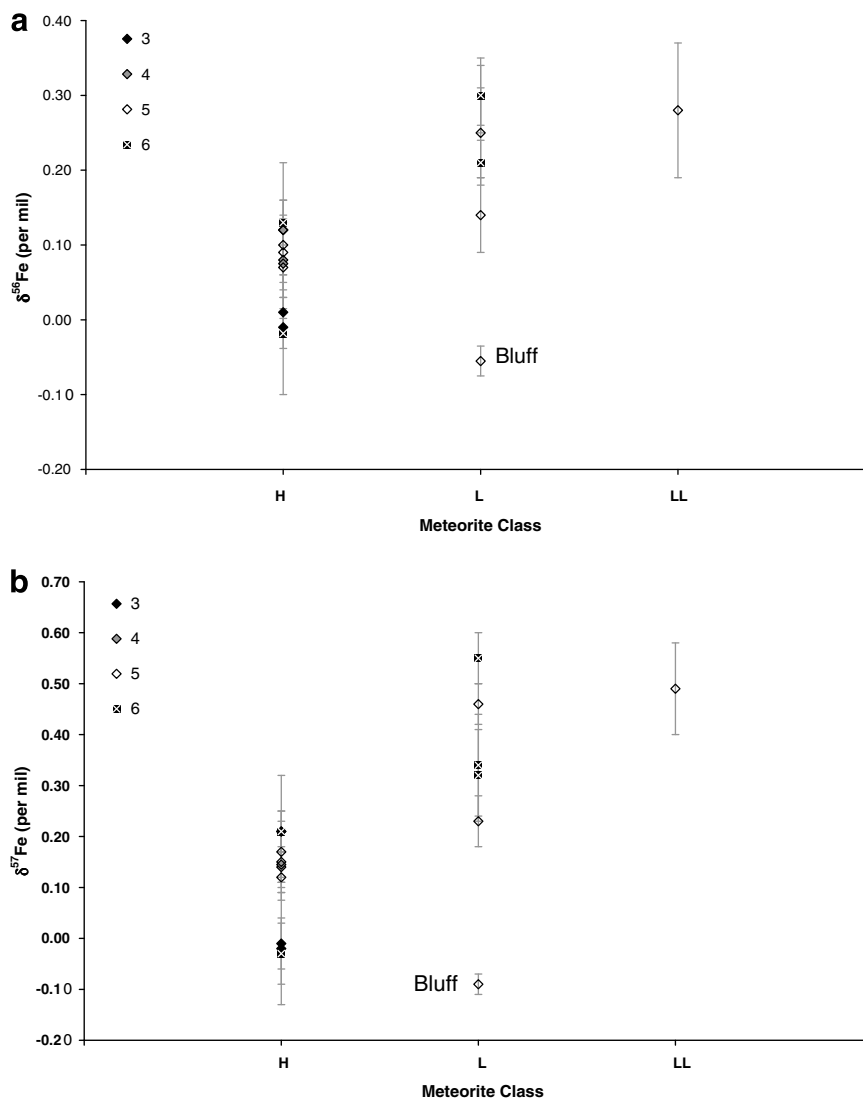
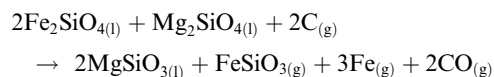


Fig. 3. Fe isotope ratios (‰) plotted as a function of meteorite classes. The data reveal a correlation between increasing oxidation state $H < L < LL$. Error bars shown to 2σ . This would suggest that the isotopic compositions are primarily determined by the chondrite and chondrule forming processes.

et al., 1988; Sears, 2004; Wlotzka, 2005; Huss et al., 2006). The highly quantitative technique of thermoluminescence enables subdivision of type 3 into 3.0–3.9, with 3.5 corresponding to a temperature of ~ 600 °C (Sears et al., 1980; Guimon et al., 1985). To quantify the amount of iron isotope fractionation that would be expected at the above closure temperatures we have used Polyakov and Mineev's (2000) data to plot the mineral fractionation factors for silicates (olivine and enstatite) and the metal iron. For petrographic type 3 with a metamorphic temperature range of between 300 and 600 °C the isotopic variation between the silicates and the metal iron (assuming the original iron reservoir was the same) should be between 0.26 and 0.10‰; for type 4 with a temperature range of 600–700 °C the variation is 0.11–0.08‰; for type 5 over the temperature range of 700–750 °C the variation is 0.09–0.07‰; and for type 6 between 750 and 950 °C the variation is 0.08 and 0.05‰.

We observe a positive correlation between enrichment of the heavier iron isotopes and increasing petrographic type (except Bluff (a)). There are several discussions in the literature stating that small changes in the oxidation state occur with increasing metamorphism, although authors disagree on whether this is due to oxidation, which is the suggested cause for changing modal abundances of olivine and pyroxene (McSween and Labotka, 1993) or reduction, as carbon is lost as CO or CO_2 (Sears and Weeks, 1983; Brett and Sato, 1984; Clayton et al., 1995):



This reaction has been linked to changes in oxygen isotope composition with metamorphism in the type 3 ordinary chondrites (Sears and Weeks, 1983; Sears and Weeks,

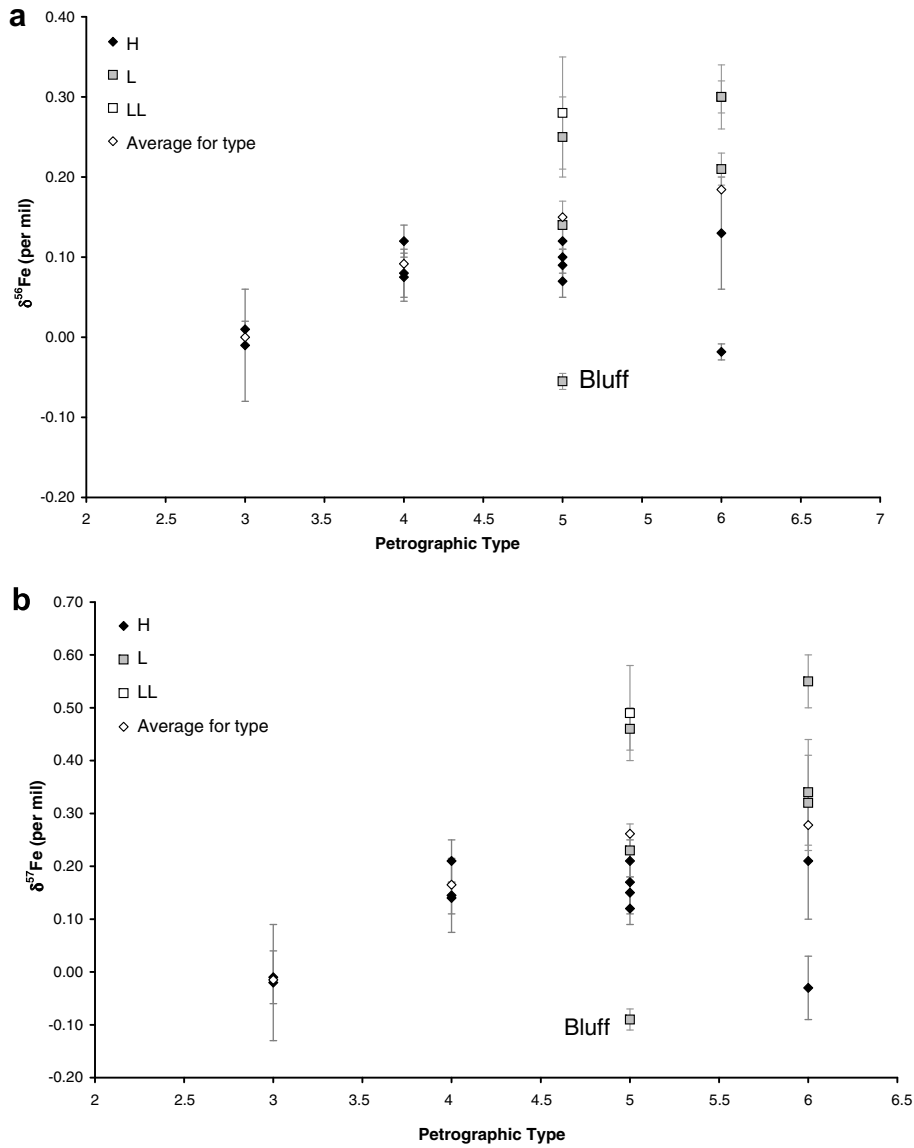


Fig. 4. Fe isotope composition plotted as a function of petrographic type (‰). Error bars (2σ) for the samples are shown as dashed grey lines whilst the error bars for the average value is shown as a solid grey line. This correlation indicates that processes occurring during metamorphism also have an effect on the isotopic composition of these samples.

1986). Thus, as with oxidative weathering, one might expect changes in iron isotope composition with petrographic type based on these reactions, however, isotopic fractionation is also a function of temperature and given that these meteorites have undergone different degrees of heating during metamorphism this may have superimposed temperature-related isotope fractionation effects on their original isotopic compositions. Fig. 6b shows that even at high temperatures where isotopic fractionation is approaching equilibrium there is still sufficient variation of between $+0.05\text{‰}$ and 0.1‰ to increase the spread of results across the different petrographic types.

Fig. 8 shows our $\delta^{56}\text{Fe}$ values plotted onto the predicted enstatite-metal iron and olivine-metal iron isotope fractionation curves using data from Polyakov and Mineev (2000).

To illustrate the petrographic correlation, the H chondrite samples, which are the most complete data set (Fig. 5), show an overall increase in $\delta^{56}\text{Fe}$ going from types 3–6. The H3 meteorites show values close to 0.0‰ equivalent to isotope temperatures $>2000\text{ °C}$. However, metamorphic temperatures for type 3 meteorites peak at $\sim 600\text{ °C}$ (McSween et al., 1988; Sears, 2004; Wlotzka, 2005; Huss et al., 2006) leading to an expected isotopic variation of around 0.1 to 0.26‰ . Clearly Fe isotope fractionation in H3 chondrites does not record metamorphic temperatures either because the temperature was not high enough to allow isotopic exchange, or the meteorites cooled too quickly to allow equilibrium fractionation. In either case it would appear that these meteorites have retained their pre-metamorphic Fe isotopic composition.

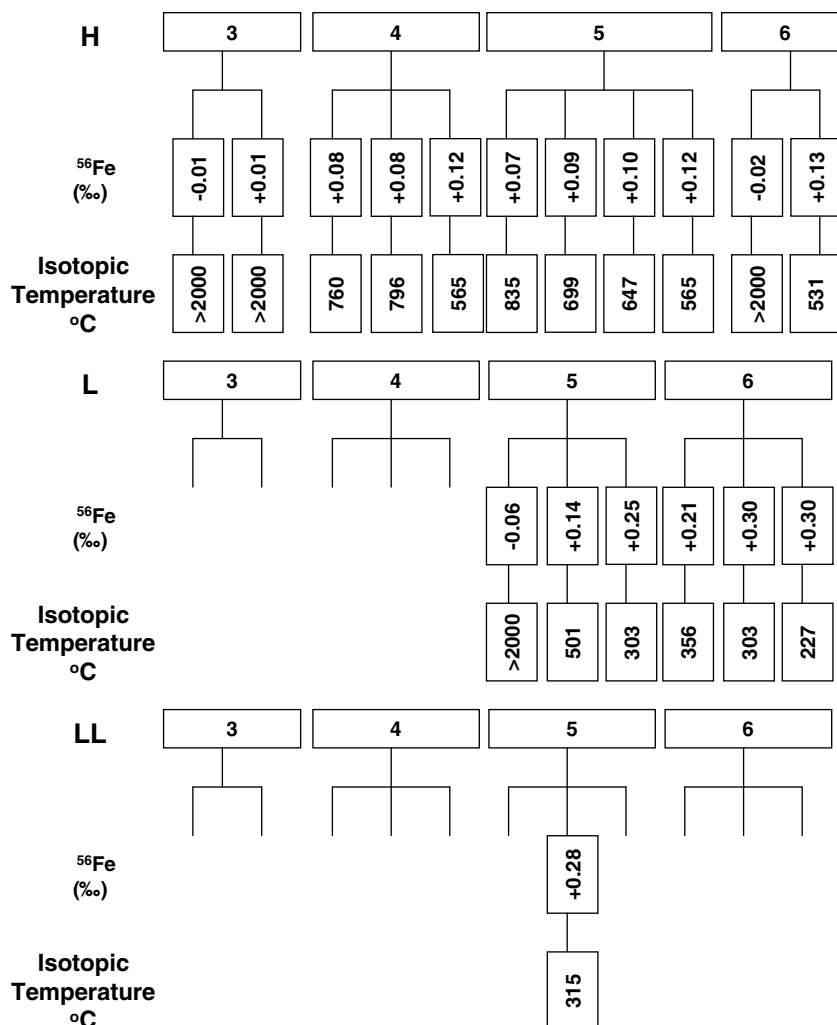


Fig. 5. Diagrammatic representation of Fe isotope composition relative to meteorite class and petrographic type. The isotopic ratios of the meteorite samples have been organised according to meteorite class and petrographic type to show that the isotopic values increase as the petrographic type increases and also as the meteorite classes' grade from H to L to LL. The temperatures shown for each sample correspond to the isotopic temperature taken from (Polyakov and Mineev, 2000) and are based on mineral-mineral isotope fractionations as a function of temperature. Hanging branches reflect gaps in the data for that particular meteorite class and petrographic type.

For the H4 ($\delta^{56}\text{Fe} = 0.08$ to 0.12‰) and the H5 ($\delta^{56}\text{Fe} = 0.07$ to 0.12‰) chondrites the isotopic temperatures are $560\text{--}800\text{ °C}$ and $560\text{--}850\text{ °C}$, respectively, which is in reasonable agreement with the literature values of $600\text{--}750\text{ °C}$ (McSween et al., 1988; Sears, 2004; Wlotzka, 2005; Huss et al., 2006). For the two type H6 chondrites ($\delta^{56}\text{Fe} = -0.02$ and 0.13‰) the correlation with metamorphic temperatures is not as clear because Kernouve (-0.02‰) shows disequilibrium fractionation and Estacado (0.13‰) yields an Fe isotope temperature of $\sim 530\text{ °C}$. However, Kernouve has not undergone heating any higher than $\sim 700\text{ °C}$ during metamorphism (Hutchison et al., 1980) and so may retain the original nebula isotope composition similar to the type 3's whilst the temperature for Estacado may reflect a cooling temperature. Equally, if redox processes were occurring during this phase then this may also have produced a small range of original Fe isotope compositions within each meteorite class, which may have

led to Estacado having an Fe isotope ratio of around $+0.02$ to $+0.05\text{‰}$ even as the temperature began to affect the fractionation of the isotopes. The effect of this would be to reduce $\Delta^{56}\text{Fe}_{\text{mineral-metal}}$ and thus increase the temperature recorded by this meteorite.

Although we do not have a full data set for all the petrographic types of the L or the LL groups, the L meteorites (except for Bluff (a)) show fractionations for L5's of between 0.14 and 0.25‰ corresponding to temperatures of $300\text{--}500\text{ °C}$, assuming a starting composition 0.0‰ . This temperature range is lower than literature values of $\sim 700\text{ °C}$ (McSween et al., 1988; Sears, 2004; Wlotzka, 2005; Huss et al., 2006) but since there is a slight increase in Fe isotope composition going from the H to L groups resulting from reduction processes, as discussed in the previous section, the original Fe isotope composition of the L group would be $>0.0\text{‰}$ and the isotope temperatures could, therefore, be higher.

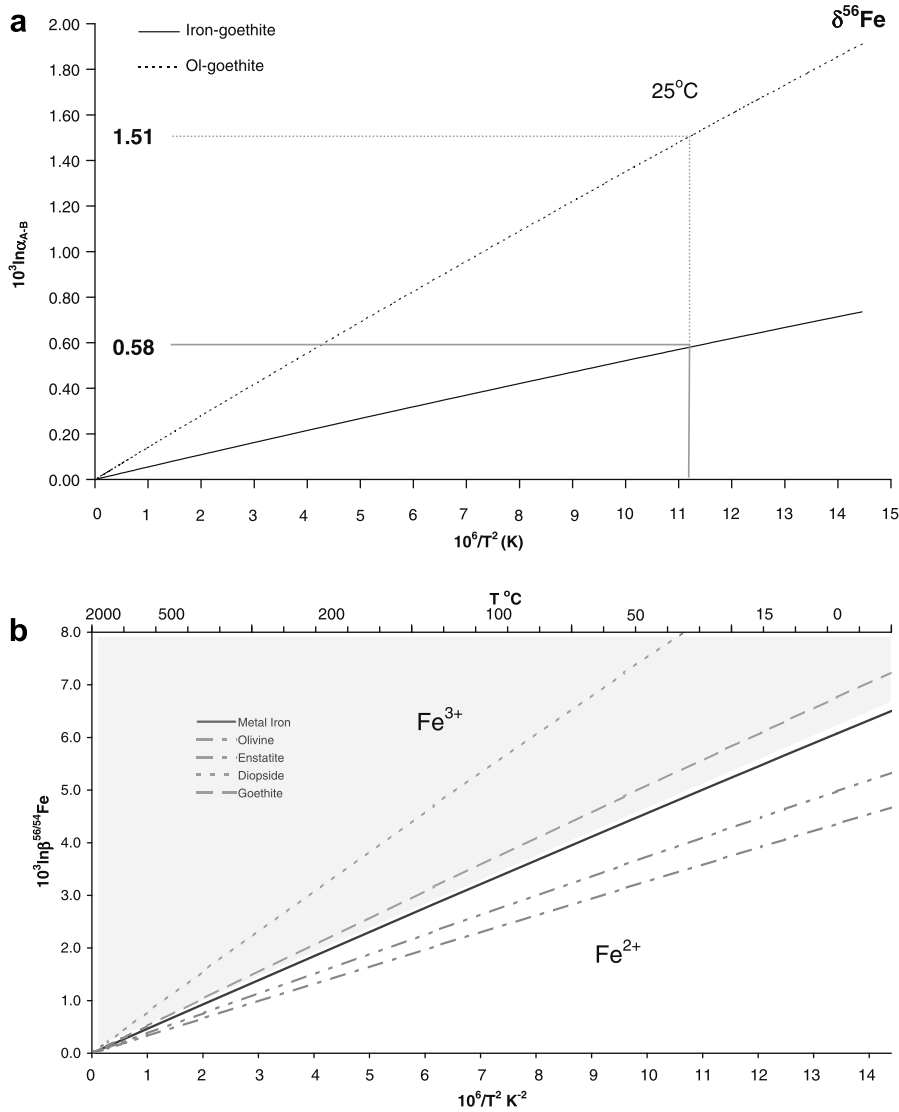


Fig. 6. Data taken from (Polyakov and Mineev, 2000). (a) shows $10^3 \ln \beta^{56/54}\text{Fe}$ plotted against temperature ($10^6/T^2 \text{ K}^{-2}$) for metal-goethite and olivine-goethite mineral fractionation, illustrating the expected variation in iron isotope composition for a temperature of around 25 °C, for metal-goethite fractionation = 0.58‰ and for olivine-goethite fractionation = 1.51‰. (b) shows the expected isotopic fractionation for various Fe bearing minerals. β is defined by (Polyakov and Mineev, 2000) as the reduced isotopic partition function ratio. Temperature is also shown in degrees (°C).

The metal grains in chondrites consist essentially of kamacite (low-Ni, body-centred cubic— α -phase) and taenite (high-Ni, face-centred cubic— γ -phase). These phases are known to have isotopically distinct Fe in iron meteorites, with the Fe in kamacite being isotopically heavier than the Fe in taenite (Poitrasson et al., 2005; Needham et al., 2006). The Fe–Ni phase diagram (Owen and Liu, 1949; Goldstein and Ogilvie, 1965) shows that as the metal initially cools to sub-solidus temperatures all the metal is in the γ -phase. As it cools still further, the α -phase precipitates from the γ -phase in an amount that is determined by the bulk composition of the metal. Non-representative sampling of the two phases could affect the present data, but given that the iron isotope composition of the metal was established prior to phase

precipitation and that metal grains contained both α and γ phases, the bulk iron isotope composition is unlikely to be influenced by variations in the proportions of these phases.

4.4. Bluff (a)

Metal in Bluff (a) has unusually low $\delta^{56}\text{Fe}$ and $\delta^{57}\text{Fe}$ values (Fig. 2). At present, we do not have an explanation for these data which are based upon three repeat measurements. It is noted that Bluff (a) is highly shocked (shock stage 6 according to (McCoy et al., 1995) and heavily weathered, and it is possible that these features, or a combination of them, may have altered the original Fe isotope composition.

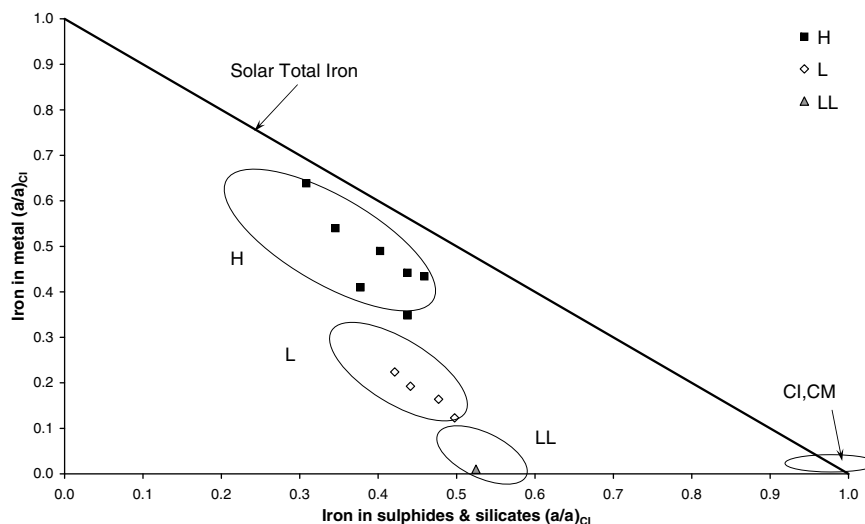


Fig. 7. Modified Urey and Craig (1953) diagram showing where the different meteorite groups plot according to (reduced) iron metal and (oxidized) iron in silicates. Six of the ordinary chondrite samples (Elm Creek, Acme, Gilgoin, Jilin, Calliham and De Nova) were not plotted as the data giving total Fe composition was unavailable. All compositional data for this plot was taken from the Metbase (meteorite database) and references are included in Table 1.

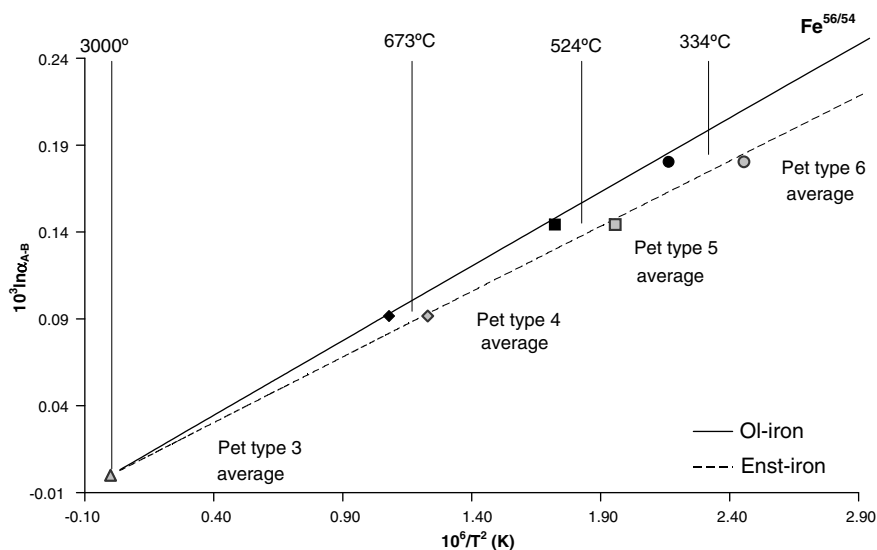


Fig. 8. Data taken from Polyakov and Mineev (2000) to show the temperature for the average isotopic ratio (which we have assumed reflects the fractionation variation of the metal iron from the silicate iron) of each petrographic type from our results based on the temperature dependant Fe isotope fractionation between metal and Fe-bearing silicates. This plot shows that the temperature indicated by the fractionation variation (0.00‰) in the type 3 meteorites reflects pre-metamorphic high temperature processes, whilst the variation for the type 4–6 meteorites reflects decreasing temperatures and, therefore, cooling rates of the metamorphic process.

4.5. Fe isotope comparison of metal, chondrules, and chondrites

In Fig. 9 we compare the present data with literature data, which mostly comprises separated chondrules, matrix samples and bulk samples. To a reasonable approximation, bulk and matrix samples have similar iron isotope compositions and are therefore grouped together for our present discussion.

Data for the H chondrites are the most complete and present the most straightforward picture, namely that

metal is enriched in the heavier isotopes of Fe, the majority of chondrules are enriched in the lighter isotopes, and bulk and matrix samples are intermediate (Fig. 9a). These data imply that there is a simple mass balance in which it is the proportion of metal and chondrules that determine the bulk composition. In this respect, the iron isotopes reflect the same processes that govern much about chondrites, i.e. that their bulk properties are a reflection of the properties and proportions of their components. But this is a simplified picture, and there is almost certainly fine detail in the components.

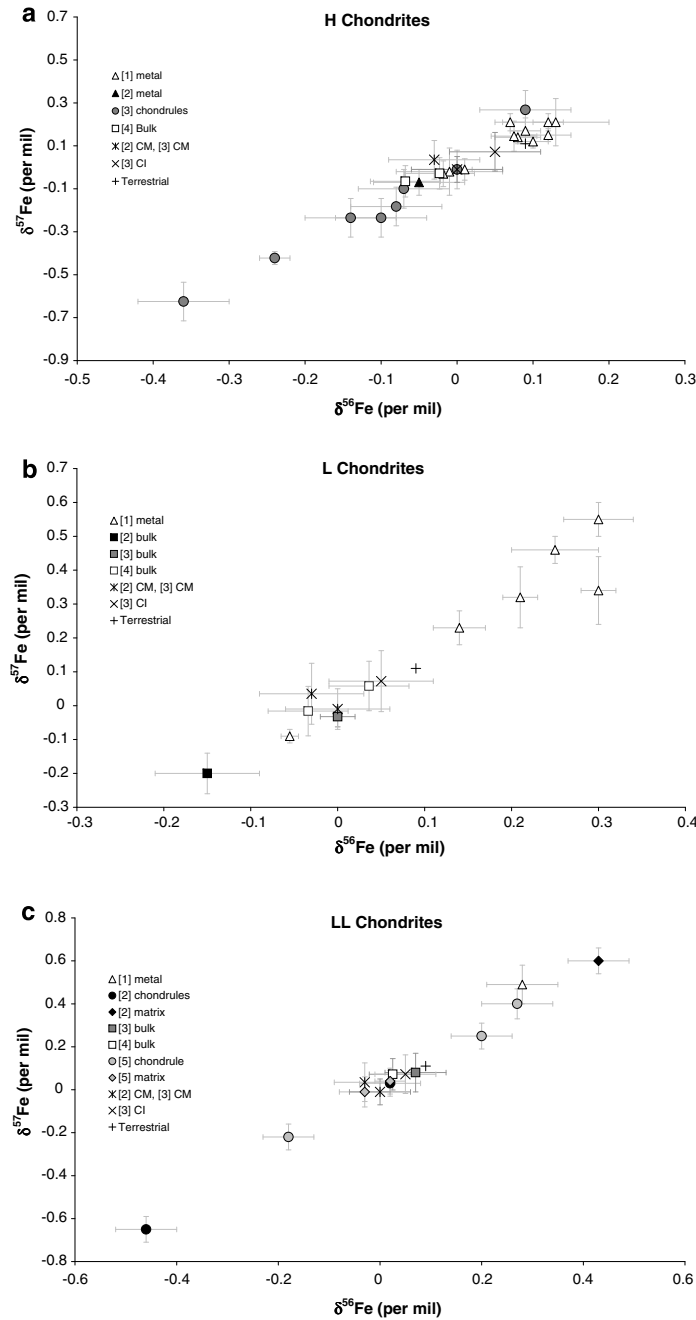


Fig. 9. Three isotope diagrams for iron isotope composition of metal grains, chondrules, matrix and bulk samples of ordinary chondrites. (a) H chondrites, comprising two H3, three H4, four H5 and two H6 chondrites (where the H3 chondrites plot at the lower end of the range), a literature value for extracted metal from an H5 (Zhu et al., 2001) and seven chondrules from Tieschitz which have lighter iron isotopic composition (Kehm et al., 2003). The $\delta^{57}\text{Fe}$ values for (Kehm et al., 2003) have been re-calculated from published $\delta^{58}\text{Fe}$ assuming mass dependant fractionation on slope of 0.75. (b) L chondrites: the present metal data for two L5 and three L6 chondrites which generally plot near the origin (Zhu et al., 2001; Schoenberg and von Blanckenburg, 2006). (c) LL chondrites, bulk and matrix samples lie in the middle of the chondrule range (aside from one matrix outlier) with our only metal sample from Aldsworth (LL5) plotting near the top of the chondrule range. Separates are from Chainpur LL3.4 (Zhu et al., 2001; Mullane et al., 2005), and bulk values are for Dar Al Garni 298 (Schoenberg and von Blanckenburg, 2006). References: [1] This study; [2] (Zhu et al., 2001) [3] (Kehm et al., 2003) [4] (Schoenberg and von Blanckenburg, 2006) [5] (Mullane et al., 2005).

Chondrules are not uniform in composition according to Mullane et al. (2005), who observed that FeO-rich chondrules are more enriched in the lighter Fe isotopes than the FeO-poor chondrules. This is also consistent with a redox control on the data.

We have no data for chondrules from L chondrites, but again the metal grains are more enriched in the heavier isotopes than the bulk samples and the bulk samples plot close to the origin in Fig. 9b. In this respect, the data for L chondrites resemble those for H chondrites.

For the LL chondrites (Fig. 9c), our single metal grain measurement is more enriched in the heavier isotopes relative to the bulk and matrix samples, and the majority of bulk and matrix samples plot near the origin, with the exception of one outlier (Zhu et al., 2001). In this respect, this class also resembles H chondrites. However, chondrules from this highly oxidized class of chondrites plot either side of the origin and overlap with our metal grain. In fact, the LL chondrites show a very large range in their level of oxidation (Sears and Axon, 1975) and some fine structure is to be expected. Further measurements should help to resolve this.

Low-FeO chondrules are those showing reduction, most probably during chondrule formation, and they will be depleted in the heavier isotopes. It is the proportion of these types of chondrule that will affect mass balance; FeO-rich chondrules will not. Most of the chondrules in LL chondrites are FeO-rich. (All of the LL chondrules from Mullane et al. (2005) are FeO-rich.)

(Cohen et al., 2006) has determined that during reduction experiments of silicate melts, kinetic isotope fractionation dominates for 60 min or so before equilibrium isotope fractionation regains control. Cohen et al. (2006) also shows an initial enrichment of ^{54}Fe in the metal iron produced from the reduced silicate melt by up to around -0.15% from the starting composition. They consider that the lighter isotope is diffused to the surface of the silicate melt and, thereby, incorporated into the iron metal, much faster than the other isotopes. These results agree with previous work carried out by Roskosz et al. (2006).

The Fe isotope composition of metal grains in ordinary chondrites show the reverse of these experiments, with metal iron grains having positive $\delta^{56}\text{Fe}$ values. Previous studies show silicates to be generally depleted in the heavier isotope. Thus, it must be assumed that equilibrium fractionation has been attained and is controlling Fe isotope partitioning during these early solar processes.

5. CONCLUSION

In this first study of the iron isotope properties of metal grains extracted from ordinary chondrites we have found that $\delta^{56}\text{Fe}$ values range from -0.06 ± 0.01 to $+0.30 \pm 0.04\%$ and $\delta^{57}\text{Fe}$ values are -0.09 ± 0.02 to $+0.55 \pm 0.05\%$ (relative to IRMM-014 iron isotope standard). There are no systematic differences in the Fe isotopes between falls and finds, although laboratory data indicates that weathering should fractionate Fe isotopes. We conclude that either these samples are only marginally weathered or that the weathering products and original metal are a closed system and sampling of the metal and weathering products was representative. $^{56}\text{Fe}/^{54}\text{Fe}$ and $^{57}\text{Fe}/^{54}\text{Fe}$ varies along the series H, L and LL in a manner expected on the basis of their differences in oxidation state. Similarly, $^{56}\text{Fe}/^{54}\text{Fe}$ and $^{57}\text{Fe}/^{54}\text{Fe}$ ratios also increase with increasing petrographic type, which again could reflect redox changes occurring during metamorphism or simple temperature dependant fractionation also during metamorphic re-heating. Metal separated from chondrites is isotopically heavier by $\sim 0.31\%$ in $^{56}\text{Fe}/^{54}\text{Fe}$ than chondrules from the same

class, while bulk and matrix samples plot between chondrules and metal. Thus, as with so many chondrite properties, the bulk values appear to reflect the proportion of chondrules (more precisely the proportion of certain types of chondrule) to metal, where chondrule properties are largely determined by chondrule formation processes.

ACKNOWLEDGMENTS

We gratefully acknowledge STFC (formerly PPARC) for providing the funding for the studentship for K.J.T. (formerly K.J. Gildea) and travel for D.W.S., and also the University of Manchester SRIF funding for the MC-ICP-MS. We thank Prof. G. Turner for helpful insights, and also C. Davies, D.J. Blagburn and B. Clementson for technical support. We also thank the suppliers of the meteorite samples listed in Table 1. We are grateful to M. Anand, E. Mullane and Nu Instruments for their technical advice and help. We are also grateful to two anonymous reviewers and the Associate Editor A. Krot for their constructive criticism which improved the paper.

REFERENCES

- Akridge D. G. and Sears D. W. G. (1999) The gravitational and aerodynamic sorting of meteoritic chondrules and metal: experimental results with implications for chondritic meteorites. *J. Geophys. Res. Planets* **104**, 11853–11864.
- Alexander C. M. O'D. and Wang J. (2001) Iron isotopes in chondrules: implications for the role of evaporation during chondrule formation. *Meteorit. Planet. Sci.* **36**, 419–428.
- Anbar A. D. (2004) Iron stable isotopes: beyond biosignatures. *Earth Planet. Sci. Lett.* **217**, 223–236.
- Anbar A. D., Roe J. E., Barling J. and Neelson K. H. (2000) Nonbiological fractionation of iron isotopes. *Science* **288**, 126–128.
- Beard B. L., Johnson C. M., Skulan J. L., Neelson K. H., Cox L. and Sun H. (2003) Application of Fe isotopes to tracing the geochemical and biological cycling of Fe. *Chem. Geol.* **195**, 87–117.
- Beard B. L. and Johnson C. M. (2004a) Fe isotope variations in the modern and ancient earth and other planetary bodies. *Geochem. Non-Traditional Stable Isotopes* **55**, 319–357.
- Beard B. L. and Johnson C. M. (2004b) Inter-mineral Fe isotope variations in mantle-derived rocks and implications for the Fe geochemical cycle. *Geochim. Cosmochim. Acta* **68**, 4727–4743.
- Belshaw N. S., Zhu X. K., Guo Y. and O'Nions R. K. (2000) High precision measurement of iron isotopes by plasma source mass spectrometry. *Int. J. Mass Spectrom.* **197**, 191–195.
- Bergquist B. A. and Boyle E. A. (2006) Iron isotopes in the Amazon River system: weathering and transport signatures. *Earth Planet. Sci. Lett.* **248**, 54–68.
- Bland P. A. (2006) Terrestrial weathering rates defined by extraterrestrial materials. *J. Geochem. Expl.* **88**, 257–261.
- Blander M. and Katz J. L. (1967) Condensation of primordial dust. *Geochim. Cosmochim. Acta* **31**, 1025–1034.
- Brett R. and Sato M. (1984) Intrinsic oxygen fugacity measurements on 7 chondrites, a pallasite, and a tektite and the redox state of meteorite parent bodies. *Geochim. Cosmochim. Acta* **48**, 111–120.
- Clayton D. D., Meyer B. S., Sanderson C. I., Russel S. S. and Pillinger C. T. (1995) Carbon and nitrogen isotopes in type II supernova diamonds. *Astrophys. J.* **447**, 894–905.
- Cohen B. A., Lévassieur S., Zanda B., Hewins R. H. and Halliday A. N. (2006) Kinetic isotope effect during reduction of iron from a silicate melt. *Geochim. Cosmochim. Acta* **70**, 3139–3148.

- Dodd R. T. (1981) *Meteorites: A Petrologic-chemical Synthesis*. Cambridge University Press.
- Dodd R. T., van Schmus W. R. and Koffman D. M. (1967) A survey of unequilibrated ordinary chondrites. *Geochim. Cosmochim. Acta* **31**, 921–951.
- Dodd R. T. (1971) Petrology of chondrules in Sharps meteorite. *Contrib. Miner. Petrol.* **31**, 201–227.
- Dodd R. T. (1976a) Accretion of ordinary chondrites. *Earth Planet. Sci. Lett.* **30**, 281–291.
- Dodd R. T. (1976b) Iron-silicate fractionation within ordinary chondrite groups. *Earth Planet. Sci. Lett.* **28**, 479–484.
- Donn B. and Sears D. W. (1963) Planets and comets—role of crystal growth in their formation. *Science* **140**, 1209–1211.
- Fantle M. S. and DePaolo D. J. (2004) Iron isotopic fractionation during continental weathering. *Earth Planet. Sci. Lett.* **228**, 547–562.
- Fodor R. V. and Keil K. (1976) Carbonaceous and non-carbonaceous lithic fragments in Plainview, Texas, chondrite—origin and history. *Geochim. Cosmochim. Acta* **40**, 177–189.
- Fredriksson K. (1963) Chondrules and meteorite parent bodies. *Trans. NY Acad. Sci.* **25**, 756–769.
- Gildea K.J., Burgess R., Lyon I.C., and Sears D.W.G. (2005) Iron isotope geochemistry of metal grains in ordinary chondrites. *Lunar Planet. Sci. XXXVI*, Lunar Planet. Inst., Houston #1668 (abstr).
- Gildea K.J., Burgess R., Lyon I., and Sears D.W. (2006) Stable iron isotope analyses of metal grains in ordinary chondrites by MC-ICP-MS. *Meteorit. Planet. Sci.* **41**, #62 (abstr).
- Gildea, K.J., Burgess, R., Lyon, I.C., and Sears, D.W.G. 2007. Stable iron isotope analyses of metal grains in ordinary chondrites by MC-ICP-MS. *Lunar Planet. Sci. XXXVIII*, Lunar Planet. Inst., Houston #1782 (abstr).
- Goldstein J. I. and Ogilvie R. E. (1965) The growth of the Widmanstätten pattern in metallic meteorites. *Geochim. Cosmochim. Acta* **29**, 893–920.
- Guimon R. K., Keck B. D., Weeks K. S., Dehart J. and Sears D. W. G. (1985) Chemical and physical studies of type 3 chondrites-IV: annealing studies of a type 3.4 ordinary chondrite and the metamorphic history of meteorites. *Geochim. Cosmochim. Acta* **49**, 1515–1524.
- Harris P. G. and Tozer D. C. (1967) Fractionation of iron in solar system. *Nature* **215**(5109), 1449–1451.
- Howard E. C. (1802) Experiments and observations on certain stony substances, which at different times are said to have fallen on the Earth; also on various kinds of native iron. *Phil. Trans.* **92**, 168–212.
- Huang S. X., Akridge G. and Sears D. W. G. (1996) Metal-silicate fractionation in the surface dust layers of accreting planetesimals: implications for the formation of ordinary chondrites and the nature of asteroid surfaces. *J. Geophys. Res. Planets* **101**, 29373–29385.
- Huss G. R., Rubin A. E. and Grossman J. N. (2006) *Thermal metamorphism in chondrites*. University of Arizona Press.
- Hutchison R. (2006) *Meteorites: A Petrologic Chemical and Isotopic Synthesis*. Cambridge University Press.
- Hutchison R., Bevan A. W. R., Easton A. J. and Agrell S. O. (1981) Mineral chemistry and genetic relations among H-Group chondrites. *Proc. Roy. Soc. Lon. A Math. Phys. Eng. Sci.* **374**, 159–178.
- Hutchison R., Bevan A. W. R., Agrell S. O. and Ashworth J. R. (1980) Thermal history of the H-group of chondritic meteorites. *Nature* **287**, 787–790.
- Jarosewich E. (1966) Chemical analyses of 10 stony meteorites. *Geochim. Cosmochim. Acta* **30**, 1261–1265.
- Jarosewich E. and Dodd R. T. (1985) Chemical variations among L-chondrites 4. Analyses, with petrographic notes, of 13I-group and 3II-group chondrites. *Meteorite* **20**, 23–36.
- Jobbins E. A., Dimes F. G., Binns R. A., Hey M. H. and Reed S. J. B. (1966) Barwell meteorite. *Mineral. Mag. J. Mineral. Soc.* **35**, 881–902.
- Johnson C. M., Skulan J. L., Beard B. L., Sun H., Nealson K. H. and Braterman P. S. (2002) Isotopic fractionation between Fe(III) and Fe(II) in aqueous solutions. *Earth Planet. Sci. Lett.* **195**, 141–153.
- Johnson C. M., Beard B. L., Beukes N. J., Klein C. and O'Leary J. M. (2003) Ancient geochemical cycling in the Earth as inferred from Fe isotope studies of banded iron formations from the Transvaal Craton. *Contrib. Mineral. Petrol.* **144**, 523–547.
- Kehm K., Hauri E. H., Alexander C. M. O'D. and Carlson R. W. (2003) High precision iron isotope measurements of meteoritic material by cold plasma ICP-MS. *Geochim. Cosmochim. Acta* **67**, 2879–2891.
- King E. A., Jarosewich E. and Brookins D. G. (1977) Petrography and chemistry of the Faucett meteorite, Buchanan County, Missouri. *Meteorite* **12**, 13–20.
- Larimer J. W. and Anders E. (1967) Chemical fractionations in meteorites. 2 Abundance patterns and their interpretation. *Geochim. Cosmochim. Acta* **31**, 1239–1270.
- Larimer J. W. and Anders E. (1970) Chemical fractionations in meteorites 3. Major element fractionations in chondrites. *Geochim. Cosmochim. Acta* **34**, 367–387.
- Mason B. and Wiik H. B. (1967) The composition of the Belly River, Bluff, Bremervorde and Madoc meteorites. *Amer. Mus. Novitates* **2280**, 19.
- McCoy T. J., Ehlmann A. J. and Keil K. (1995) The Fayette County, Texas, Meteorites. *Meteorite* **30**, 776–780.
- McSween, jr., H. Y., Sears D. W. G. and Dodd R. T. (1988) Thermal metamorphism. In *Meteorites and the Early Solar System* (eds. J. F. Kerridge and M. S. Matthews). Univ. of Arizona Press, pp. 102–113.
- McSween H. Y. and Labotka T. C. (1993) Oxidation during metamorphism of the ordinary chondrites. *Geochim. Cosmochim. Acta* **57**, 1105–1114.
- Mullane E., Russell S. S. and Gounelle M. (2005) Nebular and asteroidal modification of the iron isotope composition of chondritic components. *Earth Planet. Sci. Lett.* **239**, 203–218.
- Needham A. W., Porcelli D. and Russell S. S. (2006) Ordinary chondrites: an iron isotope study. *Meteorit. Planet. Sci.* **41**, A130.
- Orowan E. (1969) Density of Moon and nucleation of planets. *Nature* **222**, 867.
- Owen E. A. and Liu T. H. (1949) Further X-ray study of the equilibrium diagram of the iron-nickel system. *J. Iron St. Inst.* **163**, 132–137.
- Poitrasson F., Levasseur S. and Teutsch N. (2005) Significance of iron isotope mineral fractionation in pallasites and iron meteorites for the core-mantle differentiation of terrestrial planets. *Earth Planet. Sci. Lett.* **234**, 151–164.
- Poitrasson, F., Roskosz, M., Delpech, G., Gregoire, M., and Moine, B.N. 2006. Iron isotopes track planetary accretion or differentiation?. *Geochim. Cosmochim. Acta* **70**, #498 (abstr).
- Poitrasson F. (2007) Does planetary differentiation really fractionate iron isotopes? *Earth Planet. Sci. Lett.* **256**, 484–492.
- Polyakov V. B. and Mineev S. D. (2000) The use of Mossbauer spectroscopy in stable isotope geochemistry. *Geochim. Cosmochim. Acta* **64**, 849–865.
- Prior G. T. (1916) On the genetic relationship and classification of meteorites. *Mineral. Mag.* **18**, 26–44.
- Roskosz M., Luais B., Watson H. C., Toplis M. J., Alexander C. M. O'D. and Mysen B. O. (2006) Experimental quantification

- of the fractionation of Fe isotopes during metal segregation from a silicate melt. *Earth Planet. Sci. Lett.* **248**, 851–867.
- Rowe P. N., Nienow A. W. and Agbim A. J. (1972) Preliminary quantitative study of particle segregation in gas fluidized-beds—binary-systems of near spherical particles. *Trans. Inst. Chem. Eng. Chem. Eng.* **50**, 324–333.
- Rubin A. E., Rehfeldt A., Peterson E., Keil K. and Jarosewich E. (1983) Fragmental breccias and the collisional evolution of ordinary chondrite parent bodies. *Meteorite* **18**, 179–196.
- Schoenberg R. and von Blanckenburg F. (2006) Modes of planetary-scale Fe isotope fractionation. *Earth Planet. Sci. Lett.* **252**, 342–359.
- Sears D. W. G. (2004) *The origin of chondrules and chondrites*. Cambridge University Press.
- Sears D. W. and Mills A. A. (1974) Existence of 2 groups in thermoluminescence of meteorites. *Nature* **249**, 234–235.
- Sears D. W. and Axon H. J. (1975) Metal of high Co content in LL chondrites. *Meteorite* **11**, 97–100.
- Sears D. W. and Axon H. J. (1976) Ni and Co content of chondritic metal. *Nature* **260**, 34–35.
- Sears D. W. and Durrani S. A. (1980) Thermo-luminescence and the terrestrial age of meteorites—some recent results. *Earth Planet. Sci. Lett.* **46**, 159–166.
- Sears D. W., Grossman J. N., Melcher C. L., Ross L. M. and Mills A. A. (1980) Measuring metamorphic history of unequilibrated ordinary chondrites. *Nature* **287**, 791–795.
- Sears D. W. G. and Weeks K. S. (1983) Chemical and physical studies of type-3 chondrites. 2. Thermo-luminescence of 16 type-3 ordinary chondrites and relationships with oxygen isotopes. *J. Geophys. Res.* **88**, B301–B311.
- Sears D. W. G. and Weeks K. S. (1986) Chemical and physical studies of type-3 chondrites. 6. Siderophile elements in ordinary chondrites. *Geochim. Cosmochim. Acta* **50**, 2815–2832.
- Urey H. C. and Craig H. (1953) The composition of the stone meteorites and the origin of the meteorites. *Geochim. Cosmochim. Acta* **4**, 36–82.
- Van Schmus W. R. and Wood J. A. (1967) A chemical-petrologic classification for the chondritic meteorites. *Geochim. Cosmochim. Acta* **31**, 747–765.
- Wasson J. T. (1972) Formation of ordinary chondrites. *Rev. Geophys. Space Phys.* **10**, 711–759.
- Weidenschilling S. J. (1977) Aerodynamics of solid bodies in solar nebula. *Monthly Notices Roy. Astronom. Soc.* **180**, 57–70.
- Welch S. A., Beard B. L., Johnson C. M. and Braterman P. S. (2003) Kinetic and equilibrium Fe isotope fractionation between aqueous Fe(II) and Fe(III). *Geochim. Cosmochim. Acta* **67**, 4231–4250.
- Weyer S. and Schwieters J. (2003) High precision Fe isotope measurements with high mass resolution MC-ICPMS. *Int. J. Mass Spectrom.* **226**, 355–368.
- Weyer S., Anbar A. D., Brey G. P., Munker C., Mezger K. and Woodland A. B. (2005) Iron isotope fractionation during planetary differentiation. *Earth Planet. Sci. Lett.* **240**, 251–264.
- Weyer S., Anbar A. D., Brey G. P., Munker C., Mezger K. and Woodland A. B. (2007) Discussion: Fe isotope fractionation during partial melting on Earth and the current view on the Fe isotope budgets of the planets (reply to comment of F. Poitrasson and the comment of B. L. Beard and C. M. Johnson on “Iron isotope fractionation during planetary differentiation” by S. Weyer, A. D. Anbar, G. P. Brey, C. Munker, K. Mezger and A. B. Woodland). *Earth Planet. Sci. Lett.* **256**, 638–646.
- Whipple F. L. (1966) Chondrules—suggestion concerning origin. *Science* **153**, 54–56.
- Wlotzka F. (2005) Cr spinel and chromite as petrogenetic indicators in ordinary chondrites: equilibration temperatures of petrologic types 37 to 6. *Meteorit. Planet. Sci.* **40**, 1673–1702.
- Wood J. A. (1963) On the origin of chondrules and chondrites. *Icarus* **2**, 152–180.
- Yanai K., Kojima H. and Haramura H. (1995) Catalog of the Antarctic meteorites collected from December 1969 to December 1994, with special reference to those represented in the collections of the National Institute of Polar research. *Natl. Inst. Polar Res. Tokyo*, 44–76, pp. 212–213.
- Zhu X., Guo Y., Galy A., O’Nions K., Young E. and Ash R. (2000a) High precision iron isotope measurements in meteorites. *J. Conf. Abs.* **5**, 1133.
- Zhu X. K., O’Nions R. K., Guo Y. L. and Reynolds B. C. (2000b) Secular variation of iron isotopes in North Atlantic Deep Water. *Science* **287**, 2000–2002.
- Zhu X. K., Guo Y., O’Nions R. K., Young E. D. and Ash R. D. (2001) Isotopic homogeneity of iron in the early solar nebula. *Nature* **412**, 311–313.

Associate editor: Alexander N. Krot